Conductive Fiber-Based Ultrasensitive Textile Pressure Sensor for Wearable Electronics

Jaehong Lee, Hyukho Kwon, Jungmok Seo, Sera Shin, Ja Hoon Koo, Changhyun Pang, Seungbae Son, Jae Hyung Kim, Yong Hoon Jang, Dae Eun Kim, and Taeyoon Lee*

Electronic textiles (e-textiles) where various electronic elements such as sensors,[1,2] energy harvesting devices,[3] field-effect transistors,[4,5] and antennas[6] are integrated into fabrics have attracted considerable interest with the development of advanced flexible and wearable devices.[7,8] A textile-based pressure sensor, in particular, has been widely explored for a variety of applications to include caring for the elderly,[9] diagnostics,[10] monitoring patients,[8] and human motion detection[11] due to their integrability into clothes and beds. To realize the high-performance textile-based pressure sensor, various operation types of pressure sensors such as capacitive,[12,13] piezoresistive,[14–17] piezoelectric,[18,19] and optical[20,21] have been developed. Among the mentioned pressure sensor types, a capacitive pressure sensor has advantages in terms of its simple design and analysis of the devices, high sensitivity, excellent stability, and low power consumption.[22–24] The textile-based capacitive pressure sensor is generally fabricated by using two compliant conductive fabrics as electrode plates, separated by flexible dielectric spacers such as foams, fabric spacers and soft polymers.[13,25] The fabrication of large-area fabric pressure sensors has been achieved, nevertheless, it has several drawbacks, such as poor resilience, signal drift, and sensitivity due to the low electrical conductivity of the fibers and unsatisfactory mechanical property of the dielectric polymer layer.

In order to develop a high-performance textile-based pressure sensor, conductive fibers with excellent electrical conductivity and stability against external deformation are fundamentally essential.[26] To ensure the conductive fibers, various methods such as dip-coating process of carbon-based materials,[27,28] electro-[29] and electroless-plating process[30,31] have been extensively investigated. However, the aforementioned approaches are limited in their ability to obtain a superior electrical performance and stability at the same time;[8,32] metal-based conductive fibers obtained from the electro- and electroless-plating process have excellent electrical properties and poor stability, and vice versa in the case of carbon material-based conductive fibers obtained from the dip-coating process. Recently, Lee et al. demonstrated an efficient chemical solution process, which uses the chemical reduction of aluminium (Al) metal precursor composites on the fibers, forming Al nanoparticles with connections between them.[26] The chemical solution process can be useful to obtain conductive fibers with high electrical conductivity and endurance due to the connection of metal nanoparticles; however, the poor deposition efficiency of metal nanoparticles on specific polymeric fibers without surface groups able to bind metal precursors should be improved.[33]

In this research, we describe a textile-based pressure sensor with unprecedented sensitivity, excellent durability, a fast response, and a relaxation time based on highly conductive fibers coated with dielectric rubber materials. The conductive fibers were fabricated by coating poly(styrene-block-butadiene-styrene) (SBS) polymer on the surface of poly(p-phenylene terephthalamide) (Kevlar) fiber, followed by converting a huge amount of silver (Ag) ions into Ag nanoparticles directly in the SBS polymer. The obtained conductive fibers have an excellent electrical property of 0.15 Ω cm^{-1} owing to the dense electrical connection of the Ag nanoparticles and the good stability against repeated external deformations of 3 000 bending tests. By coating poly(dimethylsiloxane) (PDMS) as dielectric layers on the surface of the conductive fibers and stacking the two PDMS-coated fibers perpendicularly to each other, a capacitive type of textile pressure sensor was successfully fabricated. The obtained pressure sensor exhibited high sensitivity (0.21 kPa^{-1}), very fast response times in the millisecond range and high stability over more than 10 000 cycles. The textile-based pressure sensor could be pixelated to matrix-type pressure sensor in the form of fabrics by using a weaving method and imbedded into gloves and clothes, which were applied to control machines wirelessly as human–machine interfaces.

Figure 1a presents a schematic illustration of the fabrication procedure of conductive fibers. The procedure involves three main steps: (i) coating of SBS on the surface of Kevlar fiber, (ii) absorption of Ag precursors into the SBS layer, and (iii) reduction of the Ag precursors to form Ag nanoparticles in the SBS layers. The SBS polymer could be uniformly coated on

J. Lee, H. Kwon, Dr. J. Seo, S. Shin, Prof. T. Lee
Nanobio Device Laboratory, School of Electrical
and Electronic Engineering
Yonsei University
50 Yonsei-ro, Seodaemun-Gu, Seoul 120-749,
Republic of Korea
E-mail: taeyoon.lee@yonsei.ac.kr

J. H. Koo, Prof. C. Pang
Department of Chemical Engineering
Stanford University
Stanford, CA 94305, USA

S. Son, Prof. D. E. Kim
Biological Cybernetics, Laboratory
School of Electrical and Electronic Engineering
Yonsei University
50 Yonsei-ro, Seodaemun-gu, Seoul 120-749, Republic of Korea

J. H. Kim, Prof. Y. H. Jang
MicroMechanics, Laboratory
School of Mechanical Engineering
Yonsei University
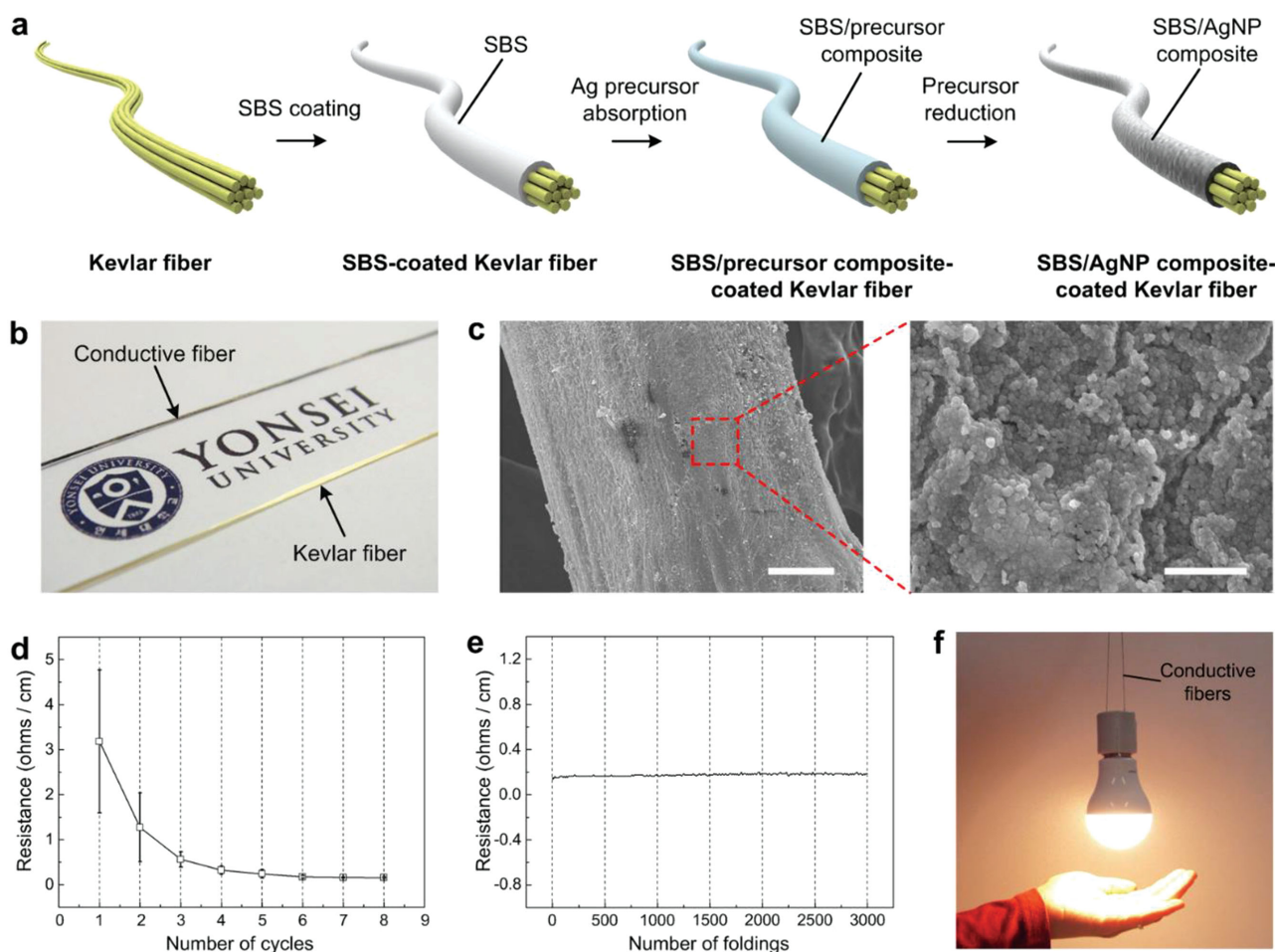50 Yonsei-ro, Seodaemun-gu, Seoul 120-749, Republic of Korea

Figure 1. a) Schematic illustration of the fabrication of a conductive fiber. b) Photograph of the fabricated conductive fiber and Kevlar fiber. c) SEM image showing the surface of the conductive fiber. (Scale bar: 50 µm) The conductive fiber is uniformly coated with the Ag nanoparticles. (The corresponding higher magnification image, Scale bar: 1 µm). d) Electrical resistance change of the conductive fiber for cycles of absorption and reduction of Ag ions; and e) during the 3 000× intensive cyclic folding test. f) Photograph showing emission of a light bulb connected to the conductive fiber.

the surface of Kevlar fiber by flowing the SBS solution along the Kevlar fiber, which was located perpendicular to the ground.[34] To absorb Ag precursors into the SBS layer, the SBS-coated fiber was immersed in a 15 wt% $AgCF_3COO$ solution in ethanol for 30 min. In this step, it is possible to achieve rapid and effective absorption of both the Ag precursors and alcoholic solvents into the SBS layer due to an ion-dipole interaction between the trifluoroacetate anions (CF_3COO^-) and hydroxyl groups (–OH) of alcoholic solvent.[35,36] To identify the absorption of precursors in the SBS layer, Fourier-transform infrared spectroscopy (FTIR) of the SBS-coated Kevlar fiber before and after the absorption of the Ag precursors was measured (Figure S1, Supporting Information). Two peaks at 1 130 and 1 184 cm^{-1} in the FTIR graph indicate the presence of the C–F stretching; this clearly reveals the absorption of the Ag precursors inside the SBS layer.[36] The absorbed Ag precursors were reduced using a solution of hydrazine hydrate ($N_2H_4 \cdot 4H_2O$), to generate Ag nanoparticles inside the SBS layer. Figure 1b provides a photograph image of the conductive fiber and Kevlar fiber, showing that the color of the conductive fiber was changed to dark grey due to the generated Ag nanoparticles on the surface of the

fiber. Figure 1c exhibits a typical scanning electron microscopy (SEM) image and a corresponding higher magnification image of the conductive fiber with a diameter of ≈320 µm. As shown in Figure 1c, the Ag nanoparticles, which were densely coated on the SBS layer with a diameter of 70–90 nm, were perfectly connected with each other. In addition to the Ag nanoparticles coated on the surface of the SBS layer, Ag precursors absorbed in the SBS layer were effectively converted to Ag nanoparticles even inside the SBS layer, resulting in excellent connections between each of the Ag nanoparticles (Figure S2, Supporting Information).

Figure 1d displays the electrical property of the conductive fiber with an electrical resistance per unit length (Ω cm^{-1}). The electrical resistance of the conductive fiber could be significantly reduced by repeating the absorption and reduction step of the Ag precursors in the SBS layer. After repeating the cycle eight times, the conductive fiber has an excellent electrical property with an electrical resistance of 0.15 Ω cm^{-1}, which is comparable with a commercialized conductive thread (1 Ω cm^{-1}) or previously reported Al threads (0.2 Ω cm^{-1}).[26] Figure S3 (Supporting Information) provides the result of the

thermogravimetric analysis, which shows the weight contents of the Ag nanoparticles in the conductive fiber. The weight contents of the Ag nanoparticles were increased from 62.8 to 82.3 wt% as the number of repeated cycles was increased. Therefore, it can be expected that the decrease in the electrical resistance of the conductive fiber after the repeated cycles is mainly attributed to the enhancement of the electrical connection of the Ag nanoparticles densely formed both inside and on the surface of the fiber. Figure 1e displays the excellent electrical stability of the conductive fiber against repeated external deformations. The external deformation involved fully folding of the conductive fiber to 180°, followed by unfolding of the fiber back to 0°. Despite 3,000 cycles of the fully folding deformation, the electrical resistance of the conductive fiber increased only by a factor of 1.25 (0.150–0.187 Ω cm^{-1}). Because the Ag nanoparticles were embedded and densely connected in the SBS layer which acts as an elastic scaffold for the Ag nanoparticles, the connection between the Ag nanoparticles could be maintained after intensively repeated bending cycles. In addition, the conductive fibers did not show any degradation in their mechanical strength and the breaking load was even slightly higher than that of the Kevlar fibers as shown in Figure S4 (Supporting Information). These results indicate that the conductive fibers have strong mechanical properties despite the intensive chemical process. Based on these outstanding electrical and mechanical properties, the conductive fibers were applied to turn on a 220 V AC light bulb safely (Figure 1f).

A capacitive type of highly sensitive textile-based pressure sensor was fabricated by coating the PDMS on the surface of the conductive fiber and stacking the PDMS-coated fibers perpendicularly to each other as shown in **Figure 2**a. The PDMS solution was uniformly coated on the surface of the conductive fiber with an average thickness of 40.5 μm by flowing the PDMS solution along the vertical conductive fiber in the same way as the SBS polymer coating. PDMS has been frequently used as an excellent dielectric material in capacitive pressure sensors in artificial skin due to its outstanding elastic properties.[24] By stacking the PDMS-coated conductive fibers perpendicularly to each other, a capacitive type of textile-based pressure sensor was formed at the cross point of the fibers. Figure 2b provides the photograph image showing the textile-based pressure sensor fabricated on a flexible poly(ethyleneterephthalate) (PET) substrate and it can be known that the textile-based pressure sensor has not only simple structure and device fabrication process but also high flexibility based on the textile materials.

Capacitance generated at the cross point of the PDMS-coated conductive fibers can be effectively changed by the incremental loads-induced thickness changing of the dielectric elastomer layer. To estimate the operation of the textile-based pressure sensor, relative changes in capacitance were measured by increasing loads of 0.05, 0.1, and 0.5 N. Figure 2c presents the capacitive response of the pressure sensor, showing that the pressure sensor has noise-free and stable continuous responses for the various loads. Figure 2d provides the response against the applied forces and relaxation properties of the pressure sensor, showing that the response to an external load was immediate and no noticeable relaxation time was observed for the loading and unloading on the pressure sensor. Significant viscoelastic behavior of the PDMS layers generally limits the performances of the capacitive pressure sensor in terms of the response and relaxation time, nevertheless, our textile-based pressure sensor exhibited very rapid response ($\approx$40 ms) and short relaxation times ($\approx$10 ms) as shown in Figure S5 (Supporting Information); this is better than those of previously reported capacitive pressure sensors for an electronic skin.[11,23,24] The rapid relaxation times result from the structure of the textile-based pressure sensor, where two PDMS-coated conductive fibers are crossed perpendicularly. The empty space
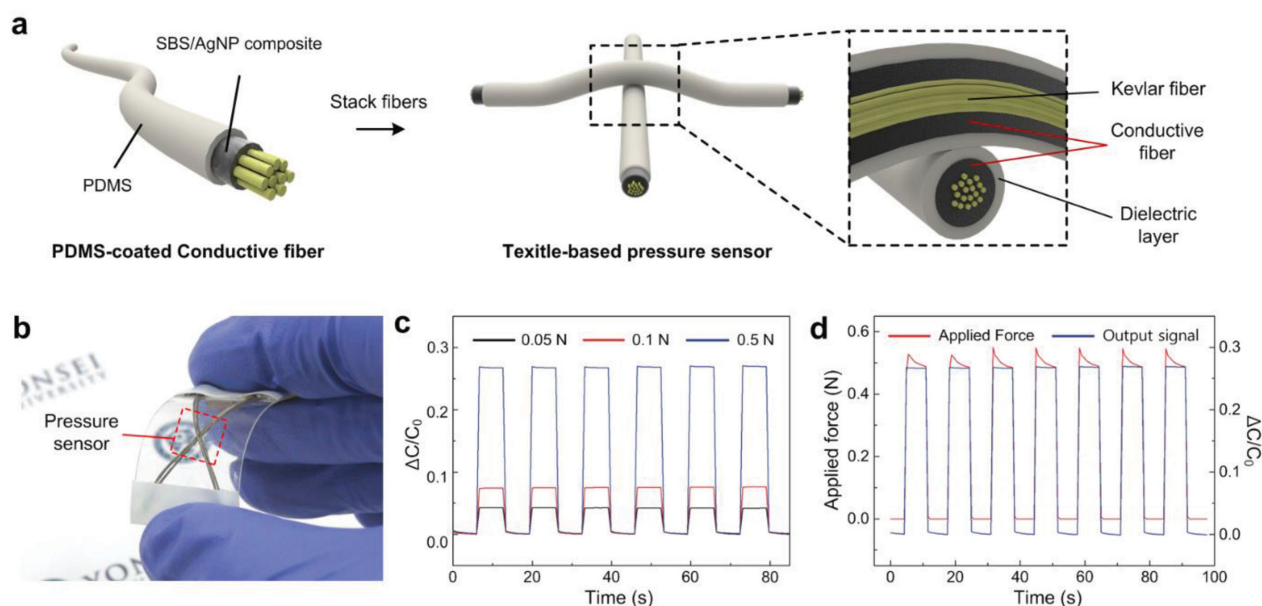

Figure 2. a) Schematic illustration of the fabrication of the pressure sensor. b) Photograph showing the fabricated pressure sensor on a PET substrate using 2 × 2 conductive fibers. c) Capacitive response of the pressure sensor for the various applied loads of 0.05, 0.1, and 0.5 N. d) Response and relaxation curve for the device under repeated application and removal of a 0.5 N load.
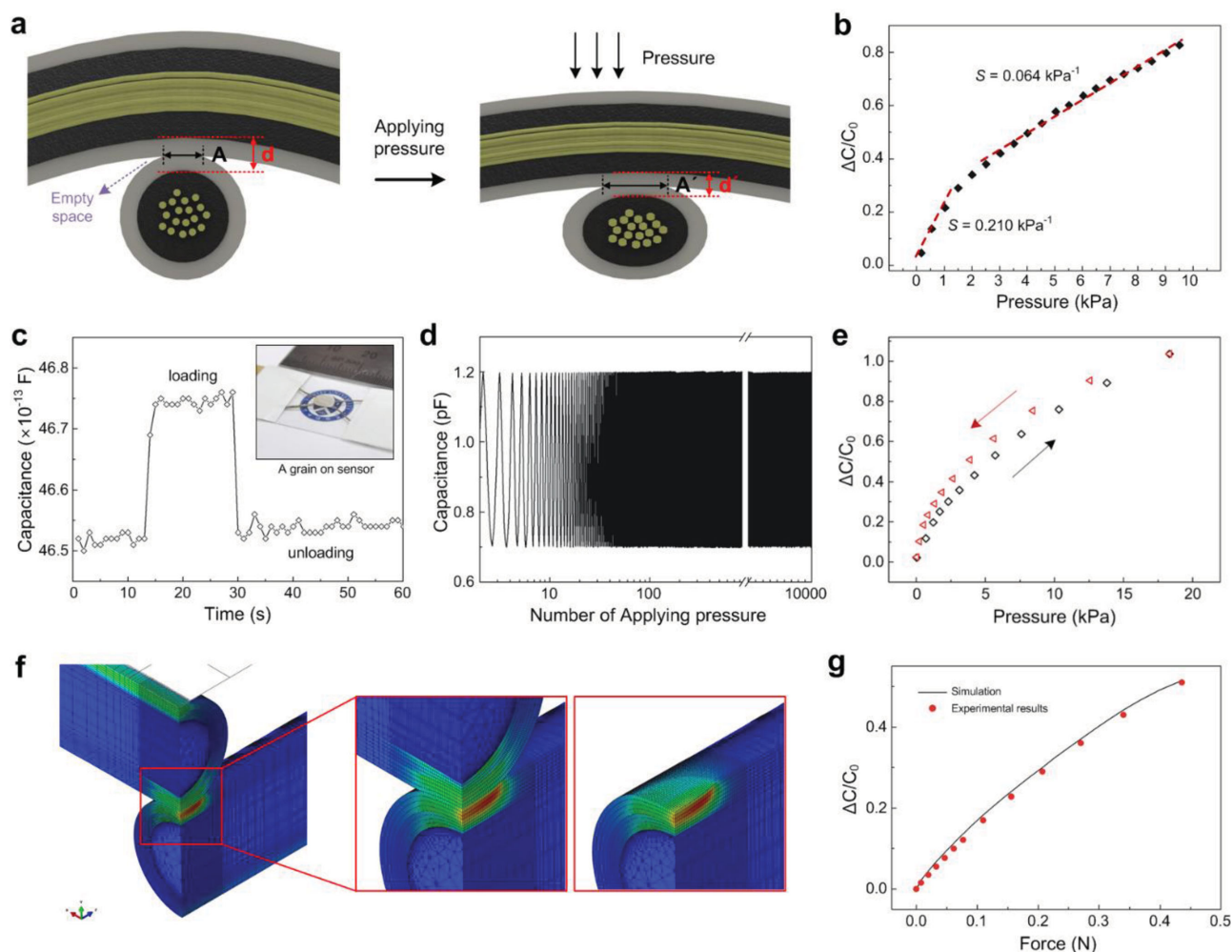
Figure 3. a) Schematic illustration showing structural change of the pressure sensor under applied pressure. This schematic shows that the contact area of the two fibers and thickness of the PDMS layers are changed at the same time after applying pressure. b) Relative capacitance change with respect to progressively increasing pressure. c) Capacitive response of the pressure sensor to the placing and removal of a grain (8 mg). The pressure sensor is successfully able to be applied to detect a very light-weight object. d) Stability of capacitive response of the pressure sensor to a load of 1.7 N over 10 000 cycles. e) Relative capacitance change of the pressure sensor from consecutive linear loading-unloading cycles of pressure. f,g) A numerical simulation of the capacitive response of the textile-based pressure sensor to increasing external forces was conducted using the finite-element method. Abaqus was used for the simulation and the contact of the upper and lower fiber was assumed to be frictionless. There is an excellent agreement between the experimental results and simulation data.

near the contact region of the two PDMS layers in the pressure sensor described in **Figure 3**a enables the PDMS layers to be effectively deformed under external pressure, resulting in storing and releasing the energy reversibly.[37] Therefore, the structure of the pressure sensor with the empty space can induce nonviscoelastic behavior of the PDMS films, leading to short relaxation times.

The sensitivity of a capacitive pressure sensor S is generally defined as $S = \delta(\Delta C/C_0)/\delta p$, where p represents the applied pressure, and C and C_0 indicate the capacitances with and without the applied pressure, respectively. The sensitivity of the textile-based pressure sensor, which can be obtained as the slope of the graph in Figure 3b, was characterized by two consecutive regions with different values. High sensitivity of 0.21 kPa^{-1} was obtained in the low pressure range under 2 kPa and there was a reduction in sensitivity to 0.064 kPa^{-1} at the pressure region above 2 kPa.

This difference between the sensitivities in the two consecutive pressure regions can be attributed to the structure in the contact area of our pressure sensor in which the fibers are crossed perpendicularly. In the low pressure region (<2 kPa), higher sensitivity could be obtained owing to the simultaneous changes in the contact area and thickness of the PDMS layers. For general capacitive pressure sensors, the related equation governing the capacitance is given by $C = \varepsilon_0 \varepsilon_r (A/d)$, where ε_0 is the space permittivity, ε_r is the relative dielectric constant of the dielectric material, A is the area of the capacitor and d is the distance between separated electrodes. In the case of our textile-based pressure sensor, two factors, (i) the area of the pressure sensor, and (ii) the distance of electrode separation, simultaneously affect the change in the capacitance as shown in Figure 3a. When the textile-based pressure sensor is compressed by external pressure, the thickness of the PDMS films,

which is directly related to the distance of electrode separation is reduced (d to d') and the contact area between the two PDMS-coated conductive fibers is increased (A to A') at the same time due to the highly deformable property of the PDMS-coated conductive fibers. Therefore, the increase in the contact area as well as the reduction in the distance between separated electrodes induces a significant increase in the capacitance of the pressure sensor under a low pressure range, inducing improvement of sensing performance compared with previously reported capacitive pressure sensors.[2,11,12] To the best of our knowledge, the sensitivity of our pressure sensor of 0.21 kPa^{-1} in the low pressure range is vastly superior to the sensitivity achieved in previously reported textile-based pressure sensors.[12,13,38] On the contrary, the sensitivity of the large pressure region was decreased to 0.064 kPa^{-1} above 2 kPa, which can be attributed to the decrease in the effective stress applied to the contact area between the two PDMS-coated conductive fibers. The increased contact area in the large pressure region induces lower effective stress than that in the low pressure region with a small contact area. Therefore, it can be expected that the decrease in the effective stress can reduce sensitivity of the pressure sensor in the large pressure region. In order to understand the behavior of the textile-based pressure sensor, a numerical simulation of the capacitive response against increasing external forces was conducted using the finite-element method as shown in Figure 3f. The details of the simulation model are described in (Figure S6, Supporting Information). The simulation result in Figure 3g shows excellent agreement with the experimental result including the change of sensitivity in the two consecutive pressure regions. Based on the excellent sensitivity, the textile-based pressure sensor could reliably detect the loading and unloading of an ultrasmall weight like a grain (weight: 8 mg) as shown in Figure 3c. In addition, the pressure sensor has a high maximum detection limit of 3.9 MPa as described in Figure S7 (Supporting Information) and it is expected that it can be improved by increasing the thickness of the PDMS layer in the pressure sensor. Furthermore, Figure S8 (Supporting Information) shows the pressure sensor exhibited a stable response for other types of mechanical forces such as bending and torsional forces.

The durability and stability of the textile-based pressure sensor were investigated through repeated loading–unloading cycling tests. As shown in Figure 3d, the output signals of the pressure sensor were stably maintained without any remarkable degradation despite intensive cycling tests that involved repeating the process 10 000 times. Therefore, it can be concluded that the textile-based pressure sensor was highly reproducible and repeatable against the repeated mechanical loads. Figure 3e also exhibits the hysteresis curves for the pressure sensor from consecutive linear loading–unloading cycles. A negligible hysteresis was observed in Figure 3e and these observations suggest that the textile-based pressure sensor has excellent durability and stability.

In order to demonstrate its ability to be applied to e-textiles applications, the textile-based pressure sensor was pixelated to a 6×6 array configuration to obtain spatial pressure information. Particularly, the array of the textile-based pressure sensor was fabricated in the form of fabrics through weaving technique. As shown in **Figure 4**a, white colored cotton fibers were used with

the PDMS-coated conductive fibers to weave the sensor array-included fabrics. The 36 pixel sensor array was fabricated with a total area of 2×1.5 cm^2 and a pixel area of $\approx$0.16 mm^2. Two light-weight beads (0.25 and 0.87 g) were located on two different sensors in the array and each small bead was carefully placed on only one pixel of pressure sensor in the fabric. The capacitive response of the pressure sensor array against the two small beads are described in Figure 4a; the pixelated sensor array was able to detect the spatial distribution of external pressure successfully. Since the resolution of the pixelated sensor array can also be controlled by changing the number of buffer fibers in the weaving process, our pixelated sensor array based on the textile-based pressure sensor has strong advantages in wearable devices or e-textile. Additionally, human motion monitoring was demonstrated by using the textile-based pressure sensor-included fabric band. When the fabric band was used as a wristband, various human hand motions such as grabbing and the opening of a hand, and the bending and unbending of a wrist were able to be detected through the capacitive response of the textile-based pressure sensor due to the contraction and relaxation of muscles as described in Figure S9 (Supporting Information).

It was demonstrated that the textile-based pressure sensor can be applied for human–machine interfaces as a real-wearable sensor platform by sewing the pressure sensors into the ends of four fingers (the index, middle, ring, and little finger) of a glove (Figure 4b) and on a forearm of clothes with 4 channels (Figure 4c). To increase robustness to parasitic capacitances from surrounding environments such as human body or clothes in the case that the sensors are used as wearable devices, the pressure sensors were fabricated using ten PDMS-coated conductive fibers to obtain a high baseline capacitance which minimizes a negative effect of parasitic capacitances. The smart glove and clothes were integrated with a custom-made data acquisition (DAQ) system with a Bluetooth communication circuit on a chip. The designed chip acquired response data from each sensors and transmitted the data to a computer wirelessly. The capacitive response of the pressure sensor was collected by measuring the rising time of charges in the capacitive pressure sensor. The capacitive response of the sensor on each finger of the glove and the forearm of clothes to external pressure is presented in Figure 4d. Each pressure sensor exhibited a sufficiently distinguishable change in capacitance without considerable interference between each sensor. Based on the performance, the wearable sensors were applied to wirelessly control a drone quadrotor (AR. Drone 2.0, Parrot SA, Paris). The four textile-based pressure sensors on the fingers of the glove were corresponded to control of the quadrotor with four different motions. (the index finger: "fly right", the middle finger: "fly forward", the ring finger: "fly left", and the little finger: "fly backward") As demonstrated in Figure 4e and Movie S1 (Supporting Information), the quadrotor could be successfully controlled with the smart glove system. In the same manner, a piece of smart clothing in which four pressure sensors were sewn on a forearm was applied to control a wired Hexapod walking robot. The four pressure sensors controlled different action commands of the robot: move backward (Channel. 1), move forward (Channel. 2), rotate counterclockwise (Channel. 3), and rotate clockwise (Channel. 4) as
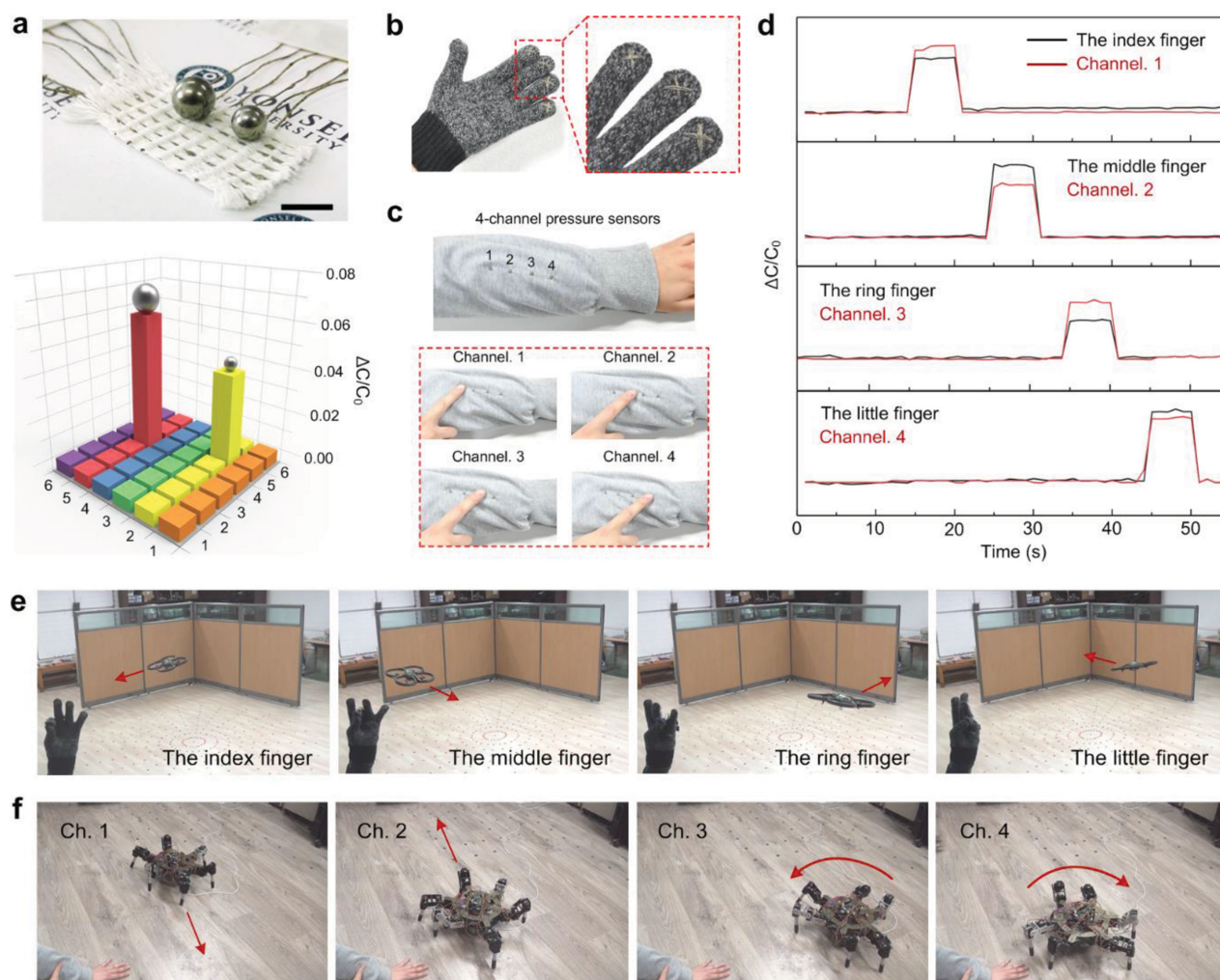
Figure 4. a) Fabrication of the pixelated pressure sensor array in fabrics to measure the spatial distribution of pressure. (Scale bar: 1 cm) b) Photograph showing the smart glove with the textile-based pressure sensors on the ends of four fingers (the index, middle, ring, and little finger) and c) clothes with 4-channel pressure sensors. d) Capacitive response of each pressure sensors in the smart glove and clothes against external pressure. e) Photographs of a remotely operated drone controlled by the smart glove; and f) a hexapod robot operated by 4-channel pressure sensors in the clothes.

described in Figure 4f and Movie S2 (Supporting Information). From these results, the textile-based pressure sensor exhibited sufficient potential for human–machine interfaces as a real-wearable sensor and it is expected that the demonstration of robot control using the smart wearable system may also be an important step for developing various unmanned aid systems.

In summary, we have developed conductive fibers with excellent electrical properties and stability, followed by fabricating a highly sensitive textile-based pressure sensor using the conductive fibers. The conductive fibers were successfully prepared by coating the elastic rubber and Ag nanoparticle composites. In addition to an excellent electrical property of 0.15 Ω cm^{-1} due to the dense electrical connection of Ag nanoparticles, the conductive fibers exhibited outstanding stability against repeated external deformations (3 000 bending tests) with the help of the elastic rubber materials which act as elastic scaffolds. By using the PDMS-coated conductive fibers, a capacitive type of textile-based pressure sensor was fabricated, which featured a high sensitivity of 0.21 kPa^{-1} in the low pressure region, fast relaxation time of less than 10 ms, excellent durability over 10 000 cycles and negligible hysteresis. The textile-based pressure sensor was integrated into a multipixel array configuration in the form of fabrics by using an weaving method, which can potentially enable us to develop highly intuitive human–machine interfaces. In addition, we demonstrated that the textile-based pressure sensor is a promising candidate for e-textiles applications by integrating the sensors into gloves and clothes to control machines wirelessly. Based on the remarkable performance of the textile-based pressure sensor, we believe that the pressure sensor will provide new opportunities for the development of real-wearable electronics in the next generation of e-textiles.

Supporting Information

Supporting Information is available from the Wiley Online Library and from the author.

COMMUNICATION

[1] C. Pang, G.-Y. Lee, T. Kim, S. M. Kim, H. N. Kim, S.-H. Ahn, K.-Y. Suh, *Nat. Mater.* **2012**, *11*, 795.

[2] D. J. Lipomi, M. Vosgueritchian, B. C.-K. Tee, S. L. Hellstrom, J. a Lee, C. H. Fox, Z. Bao, *Nat. Nanotechnol.* **2011**, *6*, 788.

[3] W. Zeng, X.-M. Tao, S. Chen, S. Shang, H. L. W. Chan, S. H. Choy, *Energy Environ. Sci.* **2013**, *6*, 2631.

[4] D. De Rossi, *Nat. Mater.* **2007**, *6*, 328.

[5] M. Hamedi, R. Forchheimer, O. Inganäs, *Nat. Mater.* **2007**, *6*, 357.

[6] R. Salvado, C. Loss, R. Gonçalves, P. Pinho, *Sensors* **2012**, *12*, 15841.

[7] D. Marculescu, R. Marculescu, N. H. Zamora, P. Stanley-marbell, S. Member, P. K. Khosla, S. Park, S. Jayaraman, S. Jung, C. Lauterbach, W. Weber, S. Member, T. Kirstein, D. Cottet, J. Grzyb, *Proc. IEEE* **2003**, *91*, 1995.

[8] P. Gould, *Mater. Today* **2003**, *6*, 38.

[9] E. R. Post, M. Orth, P. R. Russo, N. Gershenfeld, *IBM Syst. J.* **2000**, *39*, 840.

[10] P. Rai, S. Oh, P. Shyamkumar, M. Ramasamy, R. E. Harbaugh, V. K. Varadan, *J. Electrochem. Soc.* **2013**, *161*, B3116.

[11] L. Cai, L. Song, P. Luan, Q. Zhang, N. Zhang, Q. Gao, D. Zhao, X. Zhang, M. Tu, F. Yang, W. Zhou, Q. Fan, J. Luo, W. Zhou, P. M. Ajayan, S. Xie, *Sci. Rep.* **2013**, *3*, 3048.

[12] J. Meyer, B. Arnrich, *IEEE Sens. J.* **2010**, *10*, 1391.

[13] S. Takamatsu, T. Kobayashi, N. Shibayama, K. Miyake, T. Itoh, *Sens. Actuators A: Phys.* **2012**, *184*, 57.

[14] X. Wang, Y. Gu, Z. Xiong, Z. Cui, T. Zhang, *Adv. Mater.* **2014**, *26*, 1336.

[15] K. Cherenack, C. Zysset, T. Kinkeldei, N. Münzenrieder, G. Tröster, *Adv. Mater.* **2010**, *22*, 5178.

[16] M. Hussain, Y. Choa, K. Niihara, *J. Mater. Sci. Lett.* **2001**, *20*, 525.

[17] a) S. Gong, W. Schwalb, Y. Wang, Y. Chen, Y. Tang, J. Si, B. Shirinzadeh, W. Cheng, *Nat. Commun.* **2014**, *5*, 3132; b) Y. Tang, S. Gong, Y. Chen, L. W. Yap, W. Cheng, *ACS8*, 5707; c) B. Su, S. Gong, Z. Ma, L. W. Yap, W. Cheng, *Small* DOI: 10.1002/small.201403036.

[18] Y. R. Wang, J. M. Zheng, G. Y. Ren, P. H. Zhang, C. Xu, *Smart Mater. Struct.* **2011**, *20*, 045009.

[19] K. J. Kim, Y. M. Chang, S. Yoon, H. J. Kim, *Integr. Ferroelectr.* **2009**, *107*, 53.

[20] M. Rothmaier, M. P. Luong, F. Clemens, *Sensors* **2008**, *8*, 4318.

[21] S. C. Tjin, R. Suresh, N. Q. Ngo, *J. Light. Technol.* **2004**, *22*, 1728.

[22] J. A. Dobrzynska, M. A. M. Gijs, *Sens. Actuators A: Phys.* **2012**, *173*, 127.

[23] H. B. Muhammad, C. Recchiuto, C. M. Oddo, L. Beccai, C. J. Anthony, M. J. Adams, M. C. Carrozza, M. C. L. Ward, *Micro-electron. Eng.* **2011**, *88*, 1811.

[24] S. C. B. Mannsfeld, B. C.-K. Tee, R. M. Stoltenberg, C. V. H.-H. Chen, S. Barman, B. V. O. Muir, A. N. Sokolov, C. Reese, Z. Bao, *Nat. Mater.* **2010**, *9*, 859.

[25] L. M. Castano, A. B. Flatau, *Smart Mater. Struct.* **2014**, *23*, 053001.

[26] H. M. Lee, S.-Y. Choi, A. Jung, S. H. Ko, *Angew. Chem. Int. Ed. Engl.* **2013**, *52*, 7718.

[27] L. Hu, M. Pasta, F. La Mantia, L. Cui, S. Jeong, H. D. Deshazer, J. W. Choi, S. M. Han, Y. Cui, *Nano Lett.* **2010**, *10*, 708.

[28] B. S. Shim, W. Chen, C. Doty, C. Xu, N. a Kotov, *Nano Lett.* **2008**, *8*, 4151.

[29] B. K. Little, Y. Li, V. Cammarata, R. Broughton, G. Mills, *ACS Appl. Mater. Interfaces* **2011**, *3*, 1965.

[30] X. Liu, H. Chang, Y. Li, W. T. S. Huck, Z. Zheng, *ACS Appl. Mater. Interfaces* **2010**, *2*, 529.

[31] F. Ochanda, W. Jones, *Langmuir* **2005**, *21*, 10791.

[32] L. Bao, X. Li, *Adv. Mater.* **2012**, *24*, 3246.

[33] G. O. Mallory, J. B. Hajdu, William Andrew, *Electroless Plating: Fundamentals and Applications*, Orlando, Fl, USA **1991**.

[34] F. Boulogne, M. A. Fardin, S. Lerouge, L. Pauchard, F. Giorgiutti-Dauphiné, *Soft Matter* **2013**, *9*, 7787.

[35] S. F. Macha, P. A Limbach, S. D. Hanton, K. G. Owens, *J. Am. Soc. Mass Spectrom.* **2001**, *12*, 732.

[36] M. Park, J. Im, M. Shin, Y. Min, J. Park, H. Cho, S. Park, M.-B. Shim, S. Jeon, D.-Y. Chung, J. Bae, J. Park, U. Jeong, K. Kim, *Nat. Nanotechnol.* **2012**, *7*, 803.

[37] B. C.-K. Tee, A. Chortos, R. R. Dunn, G. Schwartz, E. Eason, Z. Bao, *Adv. Funct. Mater.* **2014**, *24*, 5427.

[38] W. Zeng, L. Shu, Q. Li, S. Chen, F. Wang, X.-M. Tao, *Adv. Mater.* **2014**, *26*, 5310.